Channel order in the two-channel Kondo lattice

R. Eder [1,*] and P. Wróbel [2]

[1]*Karlsruhe Institute of Technology, Institute for Quantum Materials and Technologies, D-76021 Karlsruhe, Germany*
[2]*Institute of Low Temperature and Structure Research, Polish Academy of Sciences, Okólna 2, PL-50-422 Wrocław, Poland*

We discuss the two-channel Kondo lattice model where a single localized spin per unit cell is coupled to two different conduction electron orbitals per unit cell. The calculation is done using the bond fermion formalism. For a Hamiltonian which is symmetric under exchange of the conduction channels we find a spontaneous breaking of this symmetry, i.e., the Kondo singlets are formed almost exclusively between the localized spin and only one of the two conduction orbitals. In addition to this channel-ferromagnetic phase we also find a channel-antiferromagnetic phase where the preferred conduction electron orbital alternates between sublattices. The parameter which determines the transition between these phases is the interchannel hybridization.

I. INTRODUCTION

Heavy fermion compounds are a much studied class of strongly correlated electron systems. Amongst other phenomena these compounds show a variety of phase transitions which occur as a function of temperature and some other experimental parameter, such as pressure, alloying, or magnetic field. Often the transition temperature approaches zero as a function of the second parameter, resulting in quantum critical points and superconducting domes [1], phenomena which have attracted considerable interest.

A widely studied model to describe these compounds is the Kondo lattice model (KLM), which is the strong coupling version [2] of the more realistic periodic Anderson model. It describes a single conduction band coupled to a periodic array of localized spins, each with $S = \frac{1}{2}$, by a Heisenberg-like exchange term. In actual heavy fermion compounds the localized spins correspond to the electrons in the $4f$ shell of rare earths or the $5f$ shells of actinides.

A single $S = \frac{1}{2}$ spin coupled to a conduction band forms a bound state with one conduction electron, resulting in a singlet ground state—the well-known Kondo effect. Thereby for weak coupling ($J \ll t$) the binding energy—the so-called Kondo temperature—is $k_B T_K \propto W e^{-\frac{1}{\rho J}}$, with W and ρ the bandwidth and density of states of the conduction band [3–12]. A noteworthy exact result for the *lattice system* is the fact that even for the KLM, where the f electrons are strictly localized, they do contribute to the Fermi surface volume [13] provided the system is a Fermi liquid. Approximate results for the lattice models have been obtained in mean-field approximation [14–26]. The resulting band structure is consistent with a simple hybridization picture: A dispersionless effective f band close to the Fermi energy of the decoupled conduction band hybridizes with the conduction electron band via an effective hybridization matrix element $\propto k_B T_K$ at weak coupling. This results in a Fermi surface with a volume corresponding to itinerant f electrons and the weakly dispersive "heavy" bands characteristic of heavy fermion compounds.

On the other hand, the single-band KLM is too simple to describe actual heavy fermion compounds [27]. First, such compounds usually have complicated band structures with more than one "heavy" band. Moreover, the relevant spin degree of freedom for the $4f$ or $5f$ shell is the total angular momentum **J** and a mapping to an $S = \frac{1}{2}$ spin is possible only if the crystalline electric field results in a doubly degenerate ground state. Accordingly, various variants of the KLM have been suggested [27] and here we consider one of them, the two-channel KLM [28,29].

More precisely, we consider a version with a single $S = \frac{1}{2}$ f spin and two uncorrelated conduction band orbitals per unit cell. We define $f_{i,\sigma}^{\dagger}$ to denote the creation operator for an f electron with z-spin σ in the unit cell i, and $c_{i,\alpha,\sigma}^{\dagger}$ to be the creation operator for an electron with z-spin σ in the conduction electron channel $\alpha \in \{1, 2\}$ in unit cell i. The Hamiltonian then reads $H = H_t + H_J$ whereby

$$H_t = \sum_{i,j} \sum_{\alpha,\beta} \sum_{\sigma} t_{(i,\alpha),(j,\beta)} \, c_{i,\alpha,\sigma}^{\dagger} c_{j,\beta,\sigma}, \tag{1}$$

$$H_J = \sum_{i,\alpha} J_{\alpha} \, \vec{S}_i \cdot \vec{\sigma}_{\alpha,i}. \tag{2}$$

Here $\vec{\sigma}_{\alpha,i} = \frac{1}{2} c_{\alpha,i,\sigma}^{\dagger} \, \vec{\tau}_{\sigma\sigma'} \, c_{\alpha,i,\sigma'}$ with $\vec{\tau}$ the vector of Pauli matrices, whereas $\vec{S}_i$ denotes the spin operator of the f electrons. By virtue of its derivation as a strong coupling limit, this Hamiltonian operates in the subspace of the Hilbert space with exactly one f electron per unit cell.

In writing down (2) we have neglected the possibility of interband exchange scattering, which, however, is no loss of generality. Namely dropping the site-index i from all operators for brevity, the most general exchange term at site i could be written as

$$H_J = \frac{1}{2} \sum_{\sigma,\sigma'} \vec{S} \cdot \vec{\tau}_{\sigma\sigma'} \sum_{\nu,\mu} a_{\nu,\sigma}^{\dagger} \, \tilde{J}_{\nu\mu} \, a_{\mu,\sigma'},$$

*robert.eder@kit.edu

where we have introduced the "original" fermion operators $a^\dagger_{\nu,\sigma}$. Hermiticity requires $\tilde{J}_{\nu\mu} = \tilde{J}^*_{\mu\nu}$ and we call the eigenvectors and eigenvalues of the 2×2 matrix of exchange constants v and J, respectively:

$$\sum_\mu \tilde{J}_{\nu\mu}\, v_{\mu,\alpha} = J_\alpha\, v_{\nu,\alpha}.$$

Introducing new conduction orbitals by the unitary transformation,

$$a_{\nu,\sigma} = \sum_\alpha v_{\nu,\alpha}\, c_{\alpha,\sigma} \Rightarrow c_{\alpha,\sigma} = \sum_\nu v^*_{\nu,\alpha}\, a_{\nu,\sigma},$$

the exchange term takes the form (2). Since both spin directions are transformed identically and independently, the effect on H_t is a unitary transformation of each of the 2×2 matrices $T_{i,j}$ with elements $t_{(i,\nu),(j,\mu)}$. The form (2) therefore implies no loss of generality.

We will consider the above model for a two-dimensional (2D) square lattice with periodic boundary conditions and denote the number of lattice sites by N, the number of conduction electrons in channel α by $N_{c,\alpha}$, whereas densities are denoted by $n_{c,\alpha} = N_{c,\alpha}/N$. We also introduce $n_c = n_{c,1} + n_{c,2}$ and the total number and density—including the f electrons—by N_e and n_e. Obviously $n_e = n_c + 1$.

By Fourier transform the kinetic term for the conduction electrons becomes

$$H_t = \sum_{\mathbf{k},\alpha,\sigma} \epsilon_{\mathbf{k},\alpha}\, c^\dagger_{\mathbf{k},\alpha,\sigma} c_{\mathbf{k},\alpha,\sigma}$$
$$+ \sum_{\mathbf{k},\sigma} (V_\mathbf{k}\, c^\dagger_{1,\mathbf{k},\sigma} c_{i,2,\mathbf{k},\sigma} + \text{H.c.}). \qquad (3)$$

In all that follows we will use

$$\epsilon_{\mathbf{k},\alpha} = -t_\alpha\, (\cos k_x + \cos k_y),$$
$$V_\mathbf{k} = -V\, (\cos k_x + \cos k_y).$$

The two-channel KLM has attracted considerable attention [30–39]. Here we study the lattice version of the model for conduction electron densities n_c close to unity by the bond fermion method [40–45]. This is a mean-field-like approach which cannot be expected to capture exotic physics such as non-Fermi-liquid behavior [30]. On the other hand, for the single-band KLM it has been found [43,44] that this technique reproduces quite well the antiferromagnetic phase transitions and the resulting phase diagram comprising the paramagnetic and two antiferromagnetic phases with different Fermi surface topology [46–51]. It therefore seems worthwhile to apply this method also to the two-channel version of the KLM.

II. BOND FERMION FORMALISM

The bond fermion formalism ultimately is a strong coupling approximation which should work best in the limit $J \gg t$. However, various calculations have shown [43,44] that it describes the single-band KLM quite well down to values of $J/t \sim 1$ where, for example, the magnetic phase transitions take place in the single-band KLM [43,44].

We consider the limit $J/t = \infty$ and assume prescribed values of $n_{c,1}$ and $n_{c,2}$ such that $n_{c,1} + n_{c,2} = 1$. Then, a translationally invariant state of lowest energy is

$$|\Psi_0\rangle = \prod_i |i,0\rangle,$$
$$|i,0\rangle = \frac{\cos\Theta}{\sqrt{2}}(c^\dagger_{i,1,\uparrow} f^\dagger_\downarrow - c^\dagger_{i,1,\downarrow} f^\dagger_\uparrow)|0\rangle$$
$$+ \frac{\sin\Theta}{\sqrt{2}}(c^\dagger_{i,2,\uparrow} f^\dagger_\downarrow - c^\dagger_{i,2,\downarrow} f^\dagger_\uparrow)|0\rangle, \qquad (4)$$

with $n_{c,1}(\Theta) = \cos^2(\Theta)$, $n_{c,2}(\Theta) = \sin^2(\Theta)$. This state has a nonvanishing value of the channel-ferromagnetism order parameter,

$$\Psi = \langle \vec{S}_i \cdot (\vec{\sigma}_{1,i} - \vec{\sigma}_{2,i}) \rangle,$$

introduced by Hoshino *et al.* [33]. Namely for the state (4) $\Psi = -\frac{3}{4}\cos(2\Theta)$. This order parameter measures different degrees of singlet formation between the localized spin and the two channels of conduction electrons.

Next, letting $J/t \to$ finite will result in *charge fluctuations*, which means electrons are transferred between unit cells, resulting (first) in cells occupied by three electrons or a single electron. The basic idea of the bond fermion formalism is to interpret these cells with three electrons or a single electron as occupied by an electronlike or a holelike fermion and derive a Hamiltonian for these. The angle Θ then is determined by minimizing the energy. For later reference we note that the expectation value of H_J in the state $|i,0\rangle$ is

$$e_0 = -\frac{3}{4}(J_1 \cos^2(\Theta) + J_2 \sin^2(\Theta)). \qquad (5)$$

We next discuss the single-cell states with three electrons and define the following basis states with z spin $\frac{1}{2}$,

$$|i,3,1,\uparrow\rangle = c^\dagger_{i,1,\uparrow} c^\dagger_{i,2,\uparrow} f^\dagger_{i,\downarrow}|0\rangle, \qquad (6)$$
$$|i,3,2,\uparrow\rangle = c^\dagger_{i,1,\uparrow} c^\dagger_{i,2,\downarrow} f^\dagger_{i,\uparrow}|0\rangle, \qquad (7)$$
$$|i,3,3,\uparrow\rangle = c^\dagger_{i,1,\downarrow} c^\dagger_{i,2,\uparrow} f^\dagger_{i,\uparrow}|0\rangle. \qquad (8)$$

We diagonalize H_J in the basis of these states, that means we make the ansatz,

$$|i,3,\nu,\uparrow\rangle = \sum_{\lambda=1}^3 \gamma_{\nu,\lambda}|i,3,\lambda,\uparrow\rangle,$$

where the energy E_ν and coefficients $\gamma_{\nu,\lambda}$ are obtained by diagonalizing the matrix,

$$H_{3e} = \begin{pmatrix} -\frac{J_1+J_2}{4} & \frac{J_2}{2} & \frac{J_1}{2} \\ \frac{J_2}{2} & \frac{J_1-J_2}{4} & 0 \\ \frac{J_1}{2} & 0 & \frac{J_2-J_1}{4} \end{pmatrix}.$$

There are two additional states with three electrons which do not couple to the ones introduced so far:

$$|i,3,4,\uparrow\rangle = c^\dagger_{i,1,\uparrow} c^\dagger_{i,1,\downarrow} f^\dagger_{i,\uparrow}|0\rangle,$$
$$|i,3,5,\uparrow\rangle = c^\dagger_{i,2,\uparrow} c^\dagger_{i,2,\downarrow} f^\dagger_{i,\uparrow}|0\rangle, \qquad (9)$$

both of which have energy $E_\nu = 0$. Basis states with z spin $-\frac{1}{2}$ are constructed in an analogous way.

As already stated, in the bond fermion formalism a single cell i in one of the states $|i, 3, \nu, \sigma\rangle$, $\nu \in 1, 2, \ldots 5$ is considered as occupied by an electronlike fermion, created by $b_{i,\nu,\sigma}^\dagger$. The possible states of a cell with a single electron—which necessarily is the f electron due to the constraint that applies to states of the KLM—are $|i, 1, \sigma\rangle = f_{i,\sigma}^\dagger |0\rangle$. These are eigenstates of H_J with eigenvalue $E = 0$. In the bond fermion formalism, if cell i is in the state $|i, 1, \sigma\rangle$ we consider it as occupied by a holelike fermion, created by $a_{i,\sigma}^\dagger$.

Denoting the set of cells occupied by a single electron (three electrons) by S_a (S_b) and defining S_s as the complement of $S_a \cup S_b$ the correspondence between the bond fermion states and those of the true KLM is

$$\left(\prod_{i \in S_a} a_{i,\sigma_i}^\dagger\right)\left(\prod_{j \in S_b} b_{j,\nu_j,\sigma_j}^\dagger\right)|0\rangle$$

$$\rightarrow \left(\prod_{i \in S_a} |i, 1, \sigma_i\rangle\right)\left(\prod_{j \in S_b} |j, 3, \nu_j, \sigma_j\rangle\right)\left(\prod_{n \in S_s} |n, 0\rangle\right). \quad (10)$$

In other words, the cells unoccupied by fermions are considered to be "filled up" by singlets with two electrons. Operators for the bond fermions are now derived by demanding that their matrix elements between the states on the left-hand side of (10) are equal to those of the true KLM Hamiltonian between the corresponding states on the right-hand side of (10). Due to the product nature of the latter, these matrix elements are usually easy to calculate. For example, the operator for the total number of electrons (including the f electrons) becomes

$$\hat{N}_e = \sum_{i,\sigma} \left(\sum_{\nu=1}^5 b_{i,\nu,\sigma}^\dagger b_{i,\nu,\sigma} - a_{i,\sigma}^\dagger a_{i,\sigma}\right) + 2N \quad (11)$$

$$= \sum_{\mathbf{k},\sigma} \left(\sum_{\nu=1}^5 b_{\mathbf{k},\nu,\sigma}^\dagger b_{\mathbf{k},\nu,\sigma} + a_{-\mathbf{k},\bar{\sigma}} a_{-\mathbf{k},\bar{\sigma}}^\dagger\right), \quad (12)$$

whereas the number of c electrons in channel α becomes

$$\hat{N}_{c,\alpha} = \sum_{i,\sigma} \left(\sum_{\nu=1}^5 (n_{\alpha,\nu} - n_{c,\alpha}(\Theta)) b_{i,\nu,\sigma}^\dagger b_{i,\nu,\sigma}\right.$$

$$\left. - n_{c,\alpha}(\Theta) a_{i,\sigma}^\dagger a_{i,\sigma}\right) + N n_{c,\alpha}(\Theta), \quad (13)$$

with $n_{1,\nu} = (1, 1, 1, 2, 0)$, $n_{2,\nu} = (1, 1, 1, 0, 2)$. It is easily verified that $\hat{N}_{c,1} + \hat{N}_{c,2} = \hat{N}_e - N$ as it has to be.

The exchange term (2) becomes

$$H_J = \sum_{i,\sigma} \left(\sum_{\nu=1}^5 (E_\nu - e_0) b_{i,\nu,\sigma}^\dagger b_{i,\nu,\sigma} - e_0 a_{i,\sigma}^\dagger a_{i,\sigma}\right) + N e_0$$

$$= \sum_{\mathbf{k},\sigma} \left(\sum_{\nu=1}^5 (E_\nu - e_0) b_{\mathbf{k},\nu,\sigma}^\dagger b_{\mathbf{k},\nu,\sigma} + e_0 a_{-\mathbf{k},\bar{\sigma}} a_{-\mathbf{k},\bar{\sigma}}^\dagger\right)$$

$$- N e_0. \quad (14)$$

To transcribe $c_{i,\alpha,\sigma}^\dagger$ we introduce the column vector of fermion operators $\mathbf{b}_\sigma^\dagger = (b_{1,\sigma}^\dagger, b_{2,\sigma}^\dagger, b_{3,\sigma}^\dagger, b_{4,\sigma}^\dagger, b_{5,\sigma}^\dagger, a_{\bar{\sigma}})^T$ (the site

index i has been omitted for brevity) when

$$c_{i,\alpha,\sigma}^\dagger = \frac{1}{\sqrt{2}} \mathbf{v}_{\alpha,\sigma} \cdot \mathbf{b}_{i,\sigma}^\dagger. \quad (15)$$

The elements of $\mathbf{v}_{\alpha,\sigma}$ are $\langle i, 3, \nu, \sigma | c_{i,\alpha,\sigma}^\dagger | i, 0\rangle$ for the first five entries and $\langle i, 0 | c_{i,\alpha,\sigma}^\dagger | i, 1, \bar{\sigma}\rangle$ for the sixth. They are given by

$$\mathbf{v}_{1,\uparrow} = (\sin\Theta(\gamma_{\nu,1} - \gamma_{\nu,2}), -\cos\Theta, 0, \cos\Theta),$$

$$\mathbf{v}_{2,\uparrow} = (\cos\Theta(\gamma_{\nu,3} - \gamma_{\nu,1}), 0, -\sin\Theta, \sin\Theta),$$

$$\mathbf{v}_{1,\downarrow} = (\sin\Theta(\gamma_{\nu,1} - \gamma_{\nu,2}), -\cos\Theta, 0, \cos\Theta),$$

$$\mathbf{v}_{2,\downarrow} = (\cos\Theta(\gamma_{\nu,3} - \gamma_{\nu,1}), 0, -\sin\Theta, \sin\Theta). \quad (16)$$

The first entry (involving the $\gamma_{\nu,\lambda}$) actually represents the first three entries, all of which have the same form but with $\nu \in \{1, 2, 3\}$. Switching to the Fourier transform $c_{\mathbf{k},\alpha,\sigma}^\dagger$ means introducing $b_{\mathbf{k},\nu,\sigma}^\dagger$ and $a_{-\mathbf{k},\bar{\sigma}}$ and the kinetic energy becomes

$$H_t = \frac{1}{2} \sum_{\mathbf{k},\sigma} b_{\mathbf{k},\mu,\sigma}^\dagger T_{\mu,\nu}(\mathbf{k}, \sigma) b_{\mathbf{k},\nu,\sigma},$$

$$T_{\mu,\nu}(\mathbf{k}, \sigma) = \sum_\alpha \epsilon_{\mathbf{k},\alpha} v_{\mu,\alpha,\sigma} v_{\nu,\alpha,\sigma}$$

$$+ V_{\mathbf{k}} (v_{\mu,1,\sigma} v_{\nu,2,\sigma} + v_{\mu,2,\sigma} v_{\nu,1,\sigma}). \quad (17)$$

Adding (14) and (17) we obtain the complete bond fermion Hamiltonian $H(\mathbf{k}, \sigma)$. This is then diagonalized by making the *ansatz* for the quasiparticle operators,

$$\beta_{\mathbf{k},\lambda,\sigma}^\dagger = \sum_\nu \gamma_{\mathbf{k},\lambda,\nu,\sigma} b_{\mathbf{k},\nu,\sigma}^\dagger, \quad (18)$$

and demanding $[H(\mathbf{k}, \sigma), \beta_{\mathbf{k},\lambda,\sigma}^\dagger] = E_{\mathbf{k},\lambda} \beta_{\mathbf{k},\lambda,\sigma}^\dagger$. By virtue of the unitarity of (18) and the form of the operator vector $\mathbf{b}_\sigma^\dagger$ (see above) it follows that the operator of electron number (12) becomes

$$\hat{N}_e = \sum_{\mathbf{k},\lambda,\sigma} \beta_{\mathbf{k},\lambda,\sigma}^\dagger \beta_{\mathbf{k},\lambda,\sigma}.$$

This means that the quasiparticle bands have to be filled as if the localized f electrons would contribute to the Fermi surface volume, which is in agreement with both experiments on heavy fermion compounds and the exact result in Ref. [13].

We can now determine the chemical potential μ for given N_e and determine the angle Θ in (4) by minimizing the energy. To avoid numerical problems with a steplike Fermi function at $T = 0$ we rather work at a small finite temperature $\beta t = 0.001$ and compute the Helmholtz free energy $F = \langle H\rangle - TS$.

However, there is a complication regarding the number of c electrons. By a well-known sum rule the number of c electrons of channel $\alpha = 1, 2$ equals the spectral weight integrated up to the chemical potential. Using the resolution of the c operators (15) and the *ansatz* (18) this becomes (see the Appendix)

$$S_{c,\alpha} = \frac{1}{2} \sum_{\mathbf{k},\lambda,\sigma} f(E_{\mathbf{k},\lambda}) \left|\sum_\nu \gamma_{\mathbf{k},\lambda,\nu,\sigma}^* v_{\alpha,\nu,\sigma}\right|^2, \quad (19)$$

where $f(E)$ is the Fermi function. Numerical evaluation shows, however, that this is in general *not* equal to the c-electron numbers obtained by taking the expectation values

of (13). In other words, we obtain different numbers of c electrons depending on whether we count them in real space and or if we integrate the spectral weight. As discussed in detail in Ref. [40] this is a consequence of the small quasiparticle weight of the "heavy" parts of the quasiparticle bands, which in turn is a consequence of the correlated nature of the model. However, this problem can be fixed [40] by enforcing the equality of real space count (13) and spectral-weight count (19) for the c electrons by means of suitable Lagrange multipliers. This is possible because the spectral weight (19) can be represented as expectation value of the operator,

$$\hat{S}_{c,\alpha} = \frac{1}{2} \sum_{\mathbf{k},\sigma} b_{\mathbf{k},\mu,\sigma}^{\dagger} \, N_{\mu,\nu}(\mathbf{k},\sigma) \, b_{\mathbf{k},\nu,\sigma},$$

$$N_{\mu,\nu}(\mathbf{k},\sigma) = v_{\mu,\alpha,\sigma} \, v_{\nu,\alpha,\sigma}. \qquad (20)$$

As discussed in Refs. [40,43] this has the additional appealing feature that it keeps the "heavy" bands near the chemical potential of the unhybridized conduction band, which is in agreement with the hybridization picture. In the present case we define $\hat{N}_{c,\pm} = \hat{N}_{c,1} \pm \hat{N}_{c,2}$ and analogously for the "spectral weight operator" $\hat{S}$ and replace

$$H \rightarrow H - \mu(\hat{N}_e - N_e) - \lambda(\hat{S}_{c,+} - \hat{N}_e + 1) - \lambda_1(\hat{N}_{c,-} - \hat{S}_{c,-}).$$

The Lagrange multipliers λ and λ_1 are adjusted to minimize the Helmholtz free energy.

We conclude this section by a discussion of the strong points and demerits of the bond fermion formalism. As has become obvious from its derivation, it is by nature a strong-coupling approach which should work best for large J/t. It is therefore clear that the bond fermion formalism can never reproduce the energy scale of the Kondo temperature $k_B T_K \propto \exp(-\rho J)$, believed to be important in the limit $J/t \rightarrow 0$. On the other hand, previous studies for the single-channel KLM have shown [43,44] that it is reasonably reliable down to $J/t \sim 1$, in that the bond fermion formalism reproduces quite well [43] the rather intricate phase diagram of the 2D KLM in the $J - n_e$ plane [46–51]. One reason may be the following: Inspection shows that all basis states on the right-hand side of (10) comply with the requirement to have exactly one f electron per cell. On the other hand, it is clear from (10) that states where two bond fermions occupy the same cell are meaningless, which means the bond fermions have to obey the constraint that no two of them occupy the same cell. Treating them as free fermions—as is done above—this hard-core constraint is simply relaxed. On the other hand, for large J/t and conduction electron densities $n_{c,1} + n_{c,2}$ close to 1 the densities of bond fermions are small. Accordingly, the probability that two of them occupy the same site and thus violate the hard-core constraint is small as well, so that relaxing the constraint may be reasonably justified. Put another way, the bond fermion formalism trades the KLM-inherent constraint for the dense system of f electrons for the constraint on the dilute system of bond fermions, so that relaxing the constraint is probably a less severe approximation.

However, there is a problem specific to the present version of the KLM, namely we did not include states with four or five electrons in a unit cell, which clearly belong to the Hilbert space of the Hamiltonian. A reason why such states probably have small weight in the ground state is that they have higher
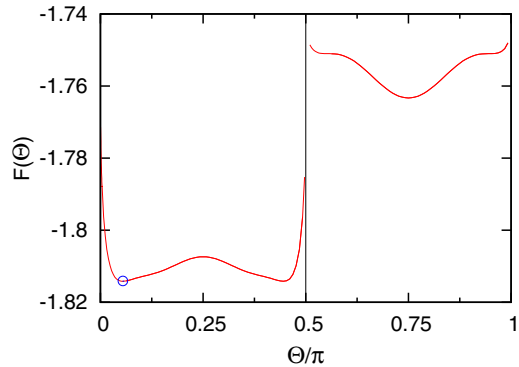

FIG. 1. Free energy versus Θ, $J = 2$, $V = 0.6$, $N_e/N = n_e = 1.9$.

energy in the limit of large J/t. Suppose we start from the product state (4) where all cells are occupied by two electrons. Then, switching on nonvanishing t produces first states with three and one electron in a cell. For large J/t their density will be small. Then, in order to create a cell with four electrons, a further electron from a cell with two electrons would have to hop into a cell with three electrons. This means, in order to create a single cell with four electrons we must create two cells with a single electron, each of which costs the energy e_0. For this reason, we expect the omitted states to have smaller weight in the ground-state wave function.

Regarding the violation of the hard-core constraint on the bond fermions, the relevance of this can be seen by calculating *a posteriori* the probability for its violation. Let n_ν be the densities of the different types (including spin) of bond fermions in the ground state. Since the bond fermions are treated as noninteracting particles the probability for violation of the hard-core constraint in the ground state is

$$p_v = 1 - \prod_\nu (1 - n_\nu) - \sum_\nu n_\nu \prod_{\mu \neq \nu} (1 - n_\mu). \qquad (21)$$

The subtracted terms are the probabilities for a given site to be empty or occupied by a single fermion. This can be easily evaluated and will be discussed below.

III. RESULTS

A. Channel-ferromagnetic phase

To begin with, we set $t_1 = t_2 = t$, as well as $J_1 = J_2 = J$, and use $t > 0$ as the unit of energy. The unhybridized conduction bands then are $\epsilon_{1,\mathbf{k}} = -(t + V)(\cos k_x + \cos k_y)$ and $\epsilon_{1,\mathbf{k}} = -(t - V)(\cos k_x + \cos k_y)$. Figure 1 shows the Helmholtz free energy F as a function of Θ. One can distinguish two regimes where the two singlets in (4) are in phase and out of phase, whereby it is obviously energetically favorable for them to be in phase. Despite the complete symmetry of the Hamiltonian under exchange of the c orbitals $\alpha = 1, 2$, the minimum of F does not occur for $\Theta = \frac{\pi}{4}$, where the two conduction bands are populated equally, but for two values symmetrically displaced with respect to $\frac{\pi}{4}$. In other words, the symmetry between the two c orbitals is spontaneously broken and the system prefers a stronger occupation of one of the two, the channel-ferromagnetic phase. This has been observed
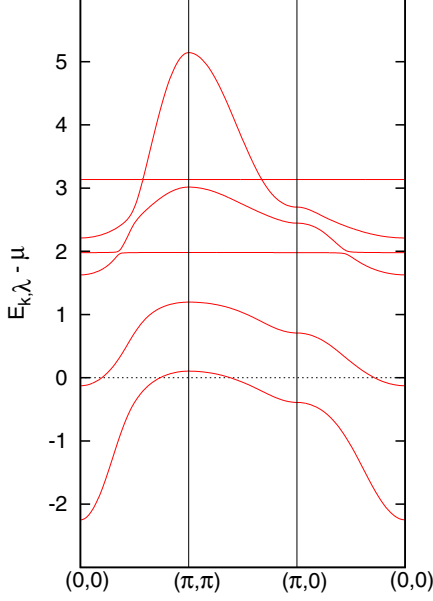
FIG. 2. Quasiparticle band structure at $\Theta_{\min}$ marked by the circle in Fig. 1.

FIG. 3. Free energy versus Θ for different J and $n_e = 1.9$.

previously by several authors [32–34,39]. However, the orbital polarization is not complete.

Figure 2 shows the band structure $E_{\mathbf{k},\lambda} - \mu$ for the parameter values in Fig. 1 at the optimal angle $\Theta_{\min}$. The six quasiparticle bands span an energy of $\approx 7.4\,t$, somewhat more than the width of the unhybridized conduction band $\epsilon_{1,\mathbf{k}}$, which is $4(t + V) = 6.4\,t$. The wave functions for the two lowest bands in the range $-2.3 < E_{\mathbf{k},\lambda} - \mu < 1.3$ have predominantly $b^\dagger_{\mathbf{k},1,\sigma}/a_{-\mathbf{k},\bar\sigma}$ character, whereas the two dispersive bands at higher energy, $1.6 < E_{\mathbf{k},\lambda} - \mu < 5.2$, are predominantly a mixture of $b^\dagger_{\mathbf{k},2,\sigma}$ and $b^\dagger_{\mathbf{k},4,\sigma}$. The flat band at $E \approx 2$ has almost pure $b^\dagger_{\mathbf{k},5,\sigma}$ character (≈ 0.95). For the small value of Θ the $\alpha = 2$ conduction electrons have negligible weight in the vacuum state $|\Psi_0\rangle$—see Eq. (4)—so that it is practically impossible to create the $b^\dagger_{\mathbf{k},5,\sigma}$ fermion by charge fluctuations; see the definition (9). The $b^\dagger_{\mathbf{k},5,\sigma}$ fermion therefore is largely decoupled and forms an isolated and essentially dispersionless band. For the $\Theta_{\min}$ close to $\frac{\pi}{2}$ in Fig. 1 the band structure is identical but the roles of $b^\dagger_{\mathbf{k},4,\sigma}$ and $b^\dagger_{\mathbf{k},5,\sigma}$ in the wave functions are interchanged. Finally, the dispersionless band at $E - \mu = 3.14$ has exclusive $b^\dagger_{\mathbf{k},3,\sigma}$ character. The corresponding eigenstate of a cell with three electrons has $S = \frac{3}{2}$ and does not couple to any of the other fermions.

For the electron density slightly less than 2 the Fermi energy cuts into the lowest band and forms an electron pocket around $(0,0)$ and a hole pocket around (π, π), whereby the effective mass around the band minimum/maximum is considerably larger than for the noninteracting band. The heavy bands known in the single-channel model thus are present also in the two-channel version.

Figure 3 shows F as a function of Θ for different values of V and J. Depending on the value of V the value of $\Theta_{\min}$—the angle where the minimum of F occurs—changes discontinuously, i.e., there is a first-order phase transition within the channel-ferromagnetic phase. For the small value $V = 0.4$,
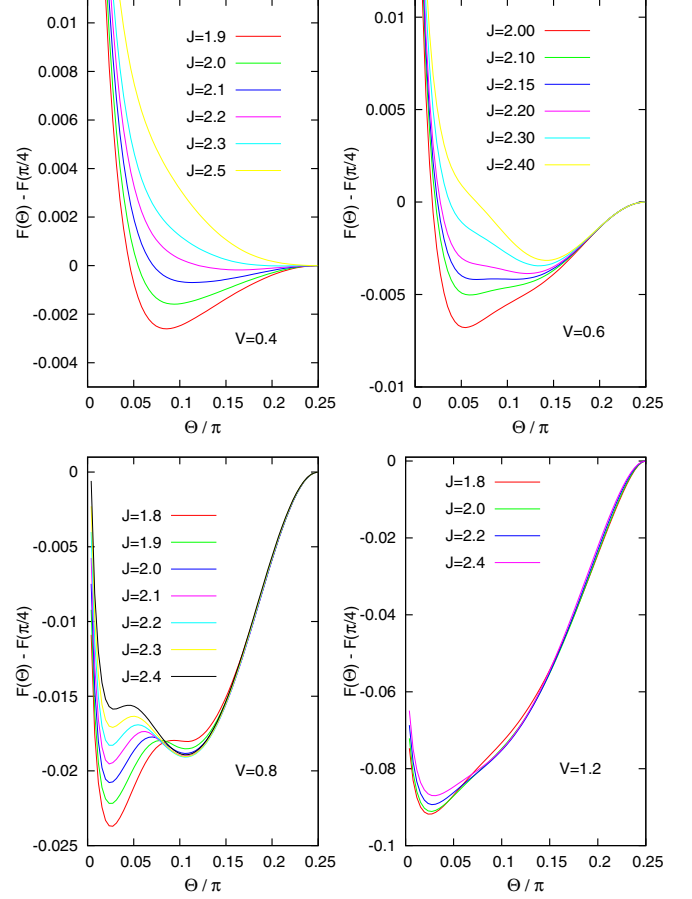
$\Theta_{\min}$ changes smoothly with J and approaches $\Theta_{\min} = \frac{\pi}{4}$ for large J, i.e., a second-order phase transition to the channel-paramagnetic phase. For $V = 0.6$ and J around $J = 2.15$ on the other hand, the curve of F versus Θ has two minima whose energies cross, resulting in a jump of $\Theta_{\min}$ from $\Theta_{\min} \approx 0.12\pi$ for larger J to $\Theta_{\min} \approx 0.025\pi$ for smaller J. This jump is even more obvious for $V = 0.8$. For the large value $V = 1.2$ on the other hand, there is only a single minimum at $\Theta_{\min} \approx 0.025$ with very little dependence on J.

To clarify the nature of the transition between the two minima, Fig. 4 shows the band structure at the respective $\Theta_{\min}$ for $V = 0.8$ and different $J = 2.0$ and $J = 2.1$. This demonstrates that the transition between the first-order phase transition in between these values of J corresponds to a Lifshitz transition where the second lowest band changes from completely unoccupied to a small hole pocket around $\mathbf{k} = (0,0)$.

Finally we consider more unsymmetric parameter sets. Figure 5 shows the free energy versus Θ for $t_1 \neq t_2$ and $J_1 \neq J_2$. As expected, asymmetry of the parameters lifts the degeneracy of the two states $\Theta_{\min} = \frac{\pi}{4} \pm \phi$ and selects a unique minimum. Interestingly, however, a relatively large asymmetry of the band parameters t_1 and t_2 has a considerably smaller impact on the energy than a small asymmetry of the exchange constants. This shows that when searching for a realization of the two-channel Kondo model and its phase transitions the closeness of the exchange constants for the two channels is most important.
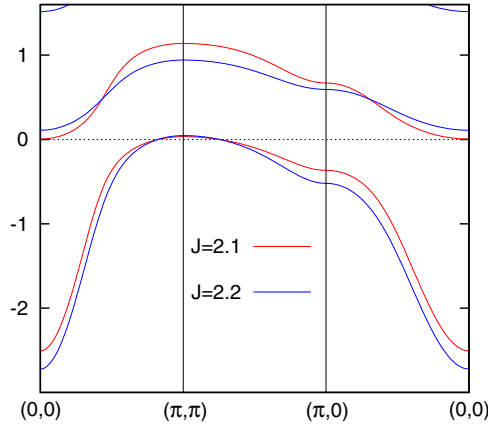
FIG. 4. The lowest two bands which form the Fermi surface for $V = 0.8$ and values of J on both sides of the transition between the two minima in Fig. 3.

B. Channel-antiferromagnetic phase

The results obtained so far suggest that the two-band Kondo model has a tendency to choose a ground state that breaks the symmetry between the two conduction bands, even in a situation where there is perfect symmetry in the Hamiltonian. One might therefore be tempted to think of a spatially inhomogeneous way to break the symmetry and the simplest way would be an "antiferromagnetic" symmetry breaking as found previously in Refs. [32,34,39]. In other words, we assume that the angle Θ in (4) varies with the site j according to $\Theta_j = \frac{\pi}{4} + e^{i\mathbf{Q}\cdot\mathbf{R}_j}\alpha$, where $\mathbf{Q} = (\pi, \pi)$, i.e., the channel-antiferromagnetic phase. We have two sublattices with angle $\Theta_j = \frac{\pi}{4} + e^{i\mathbf{Q}\cdot\mathbf{R}_j}$. Accordingly, (15) has to be replaced by

$$c_{j,\alpha,\sigma}^\dagger = \frac{1}{\sqrt{2}}\,(\mathbf{v}_{\alpha,\sigma}^{(+)} + e^{i\mathbf{Q}\cdot\mathbf{R}_j}\,\mathbf{v}_{\alpha,\sigma}^{(-)})\,\mathbf{b}_{i,\sigma}^\dagger,$$

where the two vectors $\mathbf{v}_{\alpha,\sigma}^{(\pm)}$ are symmetric and antisymmetric combinations of the respective vectors (16) for the two sublat-

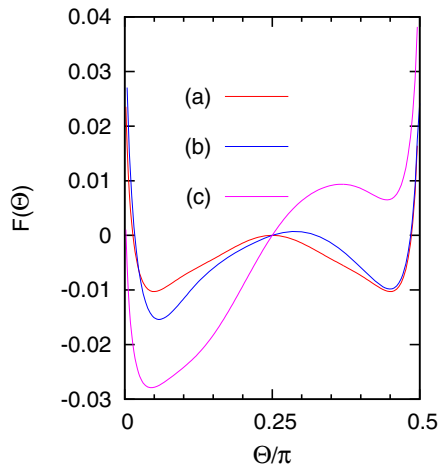FIG. 5. Ground-state energy F as a function of Θ for different "asymmetric" parameter sets: $J_1 = J_2 = 1.8$, $V = 0.6$ (a), $J_1 = J_2 = 1.8$, $V = 0.6$, $t_1 = 1$, $t_2 = 1.4$ (b), $J_1 = 1.85$, $J_2 = 1.75$, $V = 0.6$, $t_1 = t_2 = 1$ (c). Throughout $n_e = 1.9$.
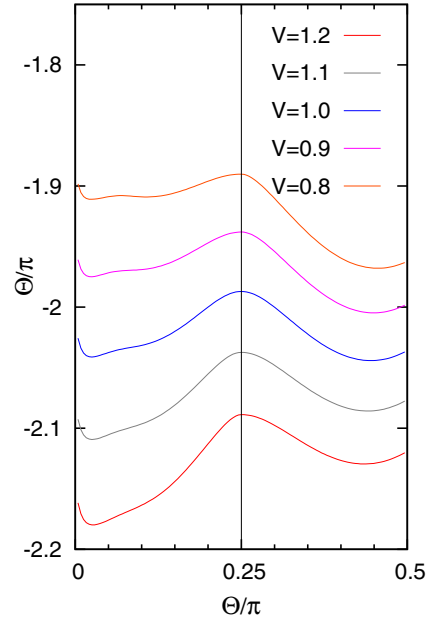

FIG. 6. Ground-state energy F versus angle Θ for the channel-ferromagnetic and channel-antiferromagnetic phases for different V. For $\Theta \leqslant \frac{\pi}{4}$ the figure shows F versus Θ for the channel-ferromagnetic phase as in Fig. 3. $\Theta = \frac{\pi}{4}$ means no singlet polarization. In the range $\Theta \geqslant \frac{\pi}{4}$ the Θ given is the one on the A sublattice of the channel-antiferromagnetic phase. The other parameter values are $J_1 = J_2 = 2.0$, $n_e = 1.9$.

tices. Upon Fourier transformation this becomes

$$c_{\mathbf{k},\alpha,\sigma}^\dagger = \frac{1}{\sqrt{2}}\,(\mathbf{v}_{\alpha,\sigma}^{(+)}\mathbf{b}_{\mathbf{k},\sigma}^\dagger + \mathbf{v}_{\alpha,\sigma}^{(-)}\,\mathbf{b}_{\mathbf{k}+\mathbf{Q},\sigma}^\dagger).$$

This means that we have to combine $\mathbf{b}_{\mathbf{k},\sigma}^\dagger$ and $\mathbf{b}_{\mathbf{k}+\mathbf{Q},\sigma}^\dagger$ into a vector of length 12 and diagonalize a 12×12 Hamilton matrix. Setting up this matrix is entirely analogous to the channel-ferromagnetic case so we do not give the lengthy explicit expressions but immediately proceed to a discussion of the results. Figure 6 compares the energy $F(\Theta)$ of the channel-ferromagnetic phase to that of the channel-antiferromagnetic phase. This shows that the variations of F with Θ are of comparable magnitude and that there is a level crossing from the channel-ferromagnetic phase for $V > 1$ to the channel-antiferromagnetic phase for $V < 1$. This first-order phase transition between the two phases can be seen for all dopings studied at $V \approx 1$. Figure 7 shows the phase boundary between the channel-ferromagnetic and channel-antiferromagnetic phases. The transition always occurs around $V \approx 1$, with the channel-antiferromagnetic phase realized for smaller V, and the channel-ferromagnetic phase for larger V. The slight bend in the phase boundary which becomes more pronounced with decreasing n_c is due to the Lifshitz transition (see Fig. 3) which occurs within the channel-ferromagnetic phase also for $V \approx 1$. Also shown is the critical value of the interband hybridization V_c as a function of hole concentration for different J.

Lastly, we briefly discuss the probability for a violation of the constraint. This is plotted in Fig. 8 for the channel-ferromagnetic phase with $n_c = 1.9$ as a function of of $J =$
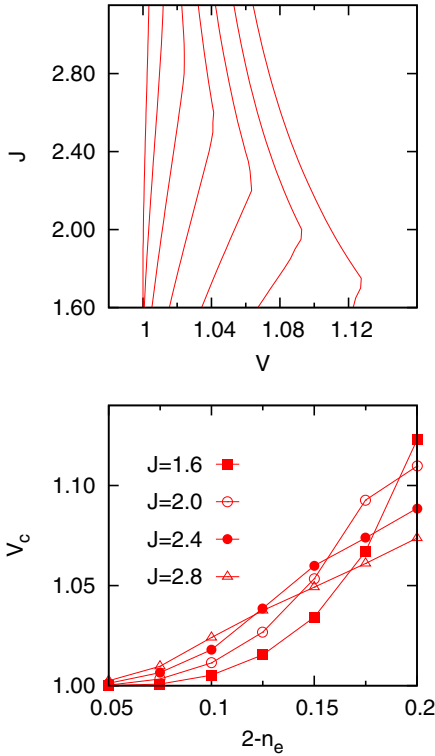
FIG. 7. (Top) Phase boundary between the channel-antiferromagnetic phase (for small V) and the channel-ferromagnetic phase (for large V). The curves refer to different electron densities, from left to right $n_e = 1.950, 1.925, 1.900, 1.875, 1.850, 1.825, 1.800$. (Bottom) Critical interband hybridization V_c as a function of hole concentration $2 - n_e$ for different J.

$J_1 = J_2$ at $\Theta_{\min}$. As expected it decreases with J, because larger J makes charge fluctuations more costly [see (14)]. It decreases with decreasing V due to the overall decrease of the kinetic energy, which prefers stronger charge fluctuations. In any way, p_v is rather small so that the approximation to relax the hard-core constraint—as was done above—seems reasonably justified.
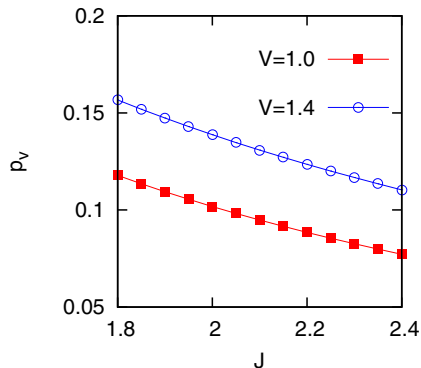

FIG. 8. Probability for violation of the constraint p_v [see Eq. (21)] for the channel-ferromagnetic phase at $n_e = 1.9$.

IV. SUMMARY AND DISCUSSION

In summary we have discussed two possible channel-ordered phases of a two-band Kondo lattice model, where a single spin-$\frac{1}{2}$ object per unit cell is exchange coupled to two conduction bands. We have found that in a situation where the Hamiltonian is symmetric under the exchange of the two conduction bands, the ground state can break this symmetry in that the localized spin forms a singlet predominantly with one of the two conduction bands. We have studied two possibilities for this symmetry breaking, namely the channel-ferromagnetic phase where one conduction band is preferred throughout the lattice, and the channel-antiferromagnetic phase where the preferred conduction channel alternates between sublattices. It turns out that the parameter which controls the transition between the two phases is mainly the interchannel hopping integral V. For small values of V the channel-antiferromagnetic phase is stable. We did not investigate the possibility of magnetic ordering, but at the large values of J/t this is not likely to play a role.

A number of previous works have studied the two-channel KLM and some of them have also studied the issue of channel order and obtained similar results. In Ref. [30] non-Fermi liquid behavior in the two-channel KLM was found by dynamical mean-field theory (DMFT). No spontaneous breaking of the symmetry between channels was considered in this study, which means the channel-paramagnetic phase was studied which appears to be unstable in the range of parameters considered in the present study. On the other hand, channel-ferromagnetic and channel-antiferromagnetic phases have been observed by several authors since then. In another DMFT study Hoshino *et al.* [33] found a channel-ferromagnetic phase. However, this was for conduction electron densities around $n_c = 2$. In this case, one of the two channels formed what could be called a single-band Kondo insulator, whereas the other channel formed a Fermi surface expected for uncoupled conduction electrons. A calculation around $n_c = 2$ which could be compared to this DMFT study is not possible within the bond fermion formalism, because—as was discussed above—the ground state of a single cell with three electrons (two conduction electrons and one f spin) is twofold degenerate so that it is not possible to write down a unique "vacuum state" for the charge fluctuations corresponding to (4) for $n_c = 1$.

Schauerte *et al.* [32] studied a one-dimensional two-channel KLM by the density matrix renormalization group method. At $n_c = 1$ and for $J/t \geqslant 2$ they found a spin-paramagnetic channel-antiferromagnetic phase, separated by a quantum-critical point from a spin-antiferromagnetic phase at smaller J/t. It is clear that magnetic phases will be suppressed by large values of J/t—as is also well established for the single-channel KLM [46–51]—so disregarding magnetic phases for the large values of J/t in the present study is probably justified.

Hoshino *et al.* [34] also studied the two-channel KLM by DMFT over a wider range of n_c. They considered a semicircular conduction band density of states of width D. For $J/t = 0.8 D$ the resulting phase diagram shows (at $T = 0$) a channel-antiferromagnetic phase in the range $0.75 < n_c < 1.25$. With our conduction electron bandwith $D = 4t$ the

value $J/t \approx 3$, roughly the range where we also found the channel-antiferromagnetic phase. No channel-ferromagnetic phase close to $n_c = 1$ was found in this study, but the Hamiltonian did not contain a mixing term for the conduction channels, i.e., $V = 0$, whereas we obtained the channel-ferromagnetic phase only for $V \geqslant 1$. The two-channel KLM was also shown to have odd-frequency pairing superconductivity [35,36] but the bond fermion method, which is very much mean-field-like, is probably too much oversimplified to address this question. Finally, both channel-ferromagnetic and channel-antiferromagnetic phases were also found in large-N approximation by Wugalter *et al.* [39]. All in all the two-channel KLM seems to have a clear tendency to spontaneous breaking of the symmetry between channels.

The two-channel KLM may have different physical realizations [29]. The first of these is the so-called quadrupolar Kondo effect [52]. Rare earth and uranium ions in the f^2 configuration, such as Pr^{3+} or U^{4+}, in cubic symmetry can have a nonmagnetic but twofold degenerate ground state, whereby the two members of the ground-state doublet differ in their electric quadrupole moment. This degree of freedom may be described by a pseudospin of $\frac{1}{2}$ and interaction with the corresponding conduction bands may be described by a Kondo-like coupling to this pseudospin. The true spin of the conduction electrons then plays the role of the channel index α. Channel order in this realization of the two-channel KLM therefore corresponds to some kind of physical spin order. However, since this order really corresponds to preferred orbital Kondo-singlet formation for one spin direction, it really takes the form of a "magnetic multipole cloud" centered around each f site which resides in the conduction electrons and hence is very extended [34].

In the second possible realization of the two-channel KLM a rare earth ion with f^1 configuration such as Ce^{3+} may undergo charge fluctuations to both an f^0 and an f^2 configuration [29]. This can also lead to a two-channel Kondo system, whereby now the localized spin indeed corresponds to the magnetic moment of the f^1 configuration. Preferred singlet formation with one of the two conduction bands might only be detected indirectly by coupling to the lattice.

APPENDIX

In this Appendix we sketch the derivation of the single-particle spectral function and expectation values of operators in the bond fermion formalism. The bond fermion Hamiltonian $H(\mathbf{k}, \sigma)$ has the form,

$$H(\mathbf{k}, \sigma) = \sum_{\mu,\nu=1}^{6} b_{\mathbf{k},\mu,\sigma}^{\dagger} h_{\mu,\nu}(\mathbf{k}, \sigma)\, b_{\mathbf{k},\nu,\sigma},$$

where the Hermitian matrix $h(\mathbf{k}, \sigma)$ can be read off from (14) and (17). This was to be diagonalized by the *ansatz* (18) for the quasiparticle operators $\beta_{\mathbf{k},\lambda,\sigma}^{\dagger}$:

$$\beta_{\mathbf{k},\lambda,\sigma}^{\dagger} = \sum_{\nu} \gamma_{\mathbf{k},\lambda,\nu,\sigma}\, b_{\mathbf{k},\nu,\sigma}^{\dagger},$$

and the requirement $[H(\mathbf{k}, \sigma), \beta_{\mathbf{k},\lambda,\sigma}^{\dagger}] = E_{\mathbf{k},\lambda} \beta_{\mathbf{k},\lambda,\sigma}^{\dagger}$. It follows that the column vector of coefficients $(\gamma_{\mathbf{k},\lambda,1,\sigma}, \gamma_{\mathbf{k},\lambda,2,\sigma}, \ldots, \gamma_{\mathbf{k},\lambda,6,\sigma})^T$ must be the eigenvector of $h(\mathbf{k}, \sigma)$ belonging to the eigenvalue $E_{\mathbf{k},\lambda}$. Therefore, (18) may be reverted as follows:

$$b_{\mathbf{k},\nu,\sigma}^{\dagger} = \sum_{\lambda} \gamma_{\mathbf{k},\lambda,\nu,\sigma}^{*}\, \beta_{\mathbf{k},\lambda,\sigma}^{\dagger},$$

and—using (15)—the physical electron operators for momentum $\mathbf{k}$, band index α, and spin σ can be expressed in terms of the quasiparticle operators as

$$c_{\mathbf{k},\alpha,\sigma}^{\dagger} = \frac{1}{\sqrt{2}} \sum_{\nu,\lambda} v_{\nu,\alpha,\sigma}\, \gamma_{\mathbf{k},\lambda,\nu,\sigma}^{*}\, \beta_{\mathbf{k},\lambda,\sigma}^{\dagger}$$

$$= \frac{1}{\sqrt{2}} \sum_{\lambda} m_{\alpha,\lambda}\, \beta_{\mathbf{k},\lambda,\sigma}^{\dagger}, \qquad (A1)$$

where the last line is the definition of the photoemission matrix element $m_{\alpha,\lambda}$. This form is used in Eq. (19).

Similarly, any quadratic form in the original $b_{i,\sigma}^{\dagger}$ operators can be rewritten as

$$\sum_{\mu,\nu} b_{\mathbf{k},\mu,\sigma}^{\dagger} o_{\mu,\nu}\, b_{\mathbf{k},\nu,\sigma} = \sum_{\lambda\lambda'} \beta_{\mathbf{k},\lambda,\sigma}^{\dagger} \tilde{o}_{\lambda\lambda'}\, \beta_{\mathbf{k},\lambda',\sigma}$$

$$\tilde{o}_{\lambda\lambda'} = \sum_{\mu,\nu} \gamma_{\mathbf{k},\lambda,\mu,\sigma}^{*} o_{\mu,\nu} \gamma_{\mathbf{k},\lambda',\nu,\sigma},$$

so that the thermal expectation value becomes

$$\left\langle \sum_{\mu,\nu} b_{\mathbf{k},\mu,\sigma}^{\dagger} o_{\mu,\nu}\, b_{\mathbf{k},\nu,\sigma} \right\rangle = \sum_{\lambda} \tilde{o}_{\lambda\lambda}\, f(E_{\mathbf{k},\lambda}),$$

which is used in Eq. (20).

[1] H. v. Löhneysen, A. Rosch, M. Vojta, and P. Wölfle, Rev. Mod. Phys. **79**, 1015 (2007).

[2] J. R. Schrieffer and P. A. Wolff, Phys. Rev. **149**, 491 (1966).

[3] K. Yosida, Phys. Rev. **147**, 223 (1966).

[4] A. Yoshimori and A. Sakurai, Progr. Theor. Phys. Suppl. **46**, 162 (1970).

[5] H. Keiter and J. C. Kimball, Int. J. Magn. **1**, 233 (1971).

[6] K. G. Wilson, Rev. Mod. Phys. **47**, 773 (1975).

[7] C. M. Varma and Y. Yafet, Phys. Rev. B **13**, 2950 (1976).

[8] Y. Kuramoto, Z. Phys. B **53**, 37 (1983).

[9] O. Gunnarsson and K. Schönhammer, Phys. Rev. B **28**, 4315 (1983).

[10] N. Read and D. M. Newns, J. Phys. C: Solid State Phys. **16**, 3273 (1983).

[11] N. Andrei, K. Furaya, and J. H. Lowenstein, Rev. Mod. Phys. **55**, 331 (1983).

[12] P. Coleman, Phys. Rev. B **29**, 3035 (1984).

[13] M. Oshikawa, Phys. Rev. Lett. **84**, 3370 (2000).

[14] C. Lacroix and M. Cyrot, Phys. Rev. B **20**, 1969 (1979).

[15] C. Lacroix, Solid State Commun. **54**, 991 (1985).

[16] A. Auerbach and K. Levin, Phys. Rev. Lett. **57**, 877 (1986).

[17] S. Burdin, A. Georges, and D. R. Grempel, Phys. Rev. Lett. **85**, 1048 (2000).

[18] G.-M. Zhang and L. Yu, Phys. Rev. B **62**, 76 (2000).

[19] M. Lavagna and C. Pepin, Phys. Rev. B **62**, 6450 (2000).

[20] T. Senthil, M. Vojta, and S. Sachdev, Phys. Rev. B **69**, 035111 (2004).

[21] M. Vojta, Phys. Rev. B **78**, 125109 (2008).

[22] G.-M. Zhang, Y.-H. Su, and L. Yu, Phys. Rev. B **83**, 033102 (2011).

[23] J. Nilsson, Phys. Rev. B **83**, 235103 (2011).

[24] X. Montiel, S. Burdin, C. Pepin, and A. Ferraz, Phys. Rev. B **90**, 045125 (2014).

[25] A. J. Millis and P. A. Lee, Phys. Rev. B **35**, 3394 (1987).

[26] D. M. Newns and N. Read, Adv. Phys. **36**, 799 (1987).

[27] P. Noziéres and A. Blandin, J. de Phys. **41**, 193 (1980).

[28] D. L. Cox and M. Jarrell, J. Phys.: Condens. Matter **8**, 9825 (1996).

[29] D. L. Cox and A. Zawadowski, Adv. Phys. **47**, 599 (1998).

[30] M. Jarrell, H. Pang, D. L. Cox, and K. H. Luk, Phys. Rev. Lett. **77**, 1612 (1996).

[31] M. Jarrell, H. B. Pang, and D. L. Cox, Phys. Rev. Lett. **78**, 1996 (1997).

[32] T. Schauerte, D. L. Cox, R. M. Noack, P. G. J. van Dongen, and C. D. Batista, Phys. Rev. Lett. **94**, 147201 (2005).

[33] S. Hoshino, J. Otsuki, and Y. Kuramoto, Phys. Rev. Lett. **107**, 247202 (2011).

[34] S. Hoshino, J. Otsuki, and Y. Kuramoto, J. Phys. Soc. Jpn. **82**, 044707 (2013).

[35] S. Hoshino and Y. Kuramoto, Phys. Rev. Lett. **112**, 167204 (2014).

[36] S. Hoshino, Phys. Rev. B **90**, 115154 (2014).

[37] S. Hoshino and Y. Kuramoto, J. Phys.: Conf. Ser. **592**, 012098 (2015).

[38] G. Zhang, J. S. Van Dyke, and R. Flint, Phys. Rev. B **98**, 235143 (2018).

[39] A. Wugalter, Y. Komijani, and P. Coleman, Phys. Rev. B **101**, 075133 (2020).

[40] R. Eder, O. Stoica, and G. A. Sawatzky, Phys. Rev. B **55**, R6109 (1997); R. Eder, O. Rogojanu, and G. A. Sawatzky, *ibid.* **58**, 7599 (1998).

[41] C. Jurecka and W. Brenig, Phys. Rev. B **64**, 092406 (2001).

[42] V. N. Kotov and P. Hirschfeld, Physica B: Condensed Matter **312-313**, 174 (2002).

[43] R. Eder, K. Grube, and P. Wróbel, Phys. Rev. B **93**, 165111 (2016).

[44] R. Eder and P. Wróbel, Phys. Rev. B **98**, 245125 (2018).

[45] M. Keßler and R. Eder, Phys. Rev. B **102**, 235125 (2020).

[46] F. F. Assaad, Phys. Rev. Lett. **83**, 796 (1999).

[47] H. Watanabe and M. Ogata, Phys. Rev. Lett. **99**, 136401 (2007).

[48] L. C. Martin, M. Bercx, and F. F. Assaad, Phys. Rev. B **82**, 245105 (2010).

[49] M. Z. Asadzadeh, F. Becca, and M. Fabrizio, Phys. Rev. B **87**, 205144 (2013).

[50] K. Kubo, J. Phys. Soc. Jpn. **84**, 094702 (2015).

[51] R. Peters and N. Kawakami, Phys. Rev. B **92**, 075103 (2015).

[52] D. L. Cox, Phys. Rev. Lett. **59**, 1240 (1987).